ELSEVIER

Effect of hydrophilicity on fouling of an emulsified oil wastewater with PVDF/PMMA membranes

N.A. Ochoa, M. Masuelli, J. Marchese*

Laboratorio de Ciencias de Superficies y Medios Porosos, Dpto. de Quimica, UNSL-CONICET-FONCYT, Chacabuco 917-5700-San Luis, Argentina

Abstract

Membranes with different degrees of hydrophilicity were prepared from PVDF and PMMA. The hydrophilicity was determined by using the contact angle technique. The distribution of pore radius was obtained from polydispersed solute permeation, scanning electron microscope (SEM) and hydraulic permeability. A higher hydrophilic character with the increase of PMMA in the casting solution and the appearance of larger macrovoids in the porous substructure were found without a substantial modification of the selective surface structure. However, a significant effect of compaction was evidenced due to the transmembrane pressure on membranes with high content of PMMA. An effluent from an engine factory was used to study the ultrafiltration performance of the prepared membranes. These assays show that membranes with a higher content of PMMA lead to a lower fouling.
© 2003 Elsevier B.V. All rights reserved.

Keywords: Ultrafiltration; Wastewater treatment; Hydrophilicity; Compaction

1. Introduction

Membrane fouling is determined by both the relationships between the size of solute and membrane pore size, and the solute-membrane material affinity. Thus, different ways of obtaining membranes with specific surface characteristics have been tested. It is known that oily effluents are strongly retained when membrane surfaces are hydrophobic and when proteins are purified at their isoelectric point. To that end, different methods to hydrophilize the surfaces under study have been carried out. These methods consist basically in (a) mixing polymers with different characteristics with respect to their hydrophobicity/

hydrophilicity, (b) grafting hydrophilic branches on hydrophobic polymer backbone and (c) the deposition of hydrophilic films on hydrophobic materials. In the first case, Nunes and Peinemann [1] reported asymmetric membranes for UF obtained from PVDF/PMMA without loss of retention. Pore size distribution showed a large increase in number of pores with sizes of 10–30 nm. The addition of PMMA also increases the size of finger-like cavities. Uragami et al. [2] obtained microporous membranes from PVDF/sulfonated polystyrene. Xu et al. [3] blended polyetherimide and polybenzimidazole in order to produce hollow fiber membranes using PEG 600 as additive. The addition of PBI in PEI/PEG dope solution resulted in a membrane structure change from a finger-like structure to a sponge structure. Varying the bore fluid, changes in water permeability and

___

* Corresponding author. Fax: +54-2652-430224.
E-mail address: marchese@unsl.edu.ar (J. Marchese).

oil–surfactant–water emulsion rejections were found whereas, with PBI addition a decrease of these parameters was observed. Recently, Hester and Mayes[4] have reported an immersion precipitate membrane with enhanced fouling resistance prepared from blends of PVDF and a free-radically synthesized amphiphilic comb polymer having a methacrylate backbone and poly(ethylene oxide) side chains. Separation surface porosity for comb-modified membranes is up to an order of magnitude higher than PVDF controls. Covalent immobilization of hydrophilic species onto membranes can be achieved by surface graft copolymerizations of the membranes with monomers in solution. Wang et al. [5] prepared PVDF microporous membranes with surface-immobilized poly(ethylene glycol) by argon plasma-induced grafting of PEG. The permeate flux of membranes thus treated decreased with increasing surface concentration of the grafted PEG polymer, while the pore size remained almost unchanged. Protein adsorption experiments revealed that PEG-g-PVDF membranes with a PEG graft concentration, defined as $[CO]/[CF_2]$ ratio above 3.2 exhibited good anti-fouling property. Nunes et al. [6] prepared dense hydrophilic composite membranes for ultrafiltration using asymmetric porous PVDF supports coated with a thin layer of polyether-block-polyamide copolymer. The performance of the composite membrane was comparable to the Amicon YM 30 cellulose membrane with a strong reduction of pore size. Sforça et al. [7] developed composite membranes prepared by a polycondensation reaction between trymesoylchloride and different amines inside a dense layer of poly(ethylene oxide-*b*-amide). Amines containing ethylene glycol blocks resulted in membranes with a cutoff as low as $600 \, \text{g mol}^{-1}$. Grafting and coating techniques result in surface modification of pore channels near the membrane surface only [6,8,9]. They also change the surface pore distribution [6,10]. In addition, foulant accumulation can occur within internal pore channels [11]. The blend of polymers presents the advantage of an easy preparation by the method of phase inversion. Moreover, having commercial polymer surfaces with low-cost appropriate characteristics can be obtained. The addition of a second polymer to the casting solution brings about the modification of structure characteristics of membranes, such as the appearance of macrovoids, which produce different behaviors in filtration [1]. However, there are few works dealing with both the effects of hydrophilicity when emulsions are filtrated, and fouling models and their relationship with membrane characteristics. More information has been gathered for BSA case. Mueller and Davis [12] showed that surface-modified polyethylene and polypropylene membranes have lower initial fluxes than unmodified membranes. However, the hydrophilic modified membranes demonstrated similar final fluxes and a lower percent of flux declines than that of the unmodified membranes. Marchese et al. [13] reported results when PVP is added onto casting solution on the BSA permeation in ultrafiltration membranes. The corresponding fouling mechanism and subsequent modification were analyzed when the membrane was in contact with BSA and DL-Histidine. BSA fouled non PVP membranes faster whereas DL-Histidine fouled them slower, according to the action of hydrophobic and electrostatic forces.

Considering that the effects of membrane hydrophilicity on oil-water treatment have not been thoroughly investigated, PVDF/PMMA membranes have been developed in this work. Membranes have been characterized determining their contact angle with respect to the hydrophilicity of membrane surface. The membrane structure was determined by SEM. The permselectivities of the membranes were determined by hydraulic permeability and by the distribution of pore size obtained from the permeation of dextrans. Membrane behavior in the filtration of oil–water emulsion has been evaluated by fouling model. The quality of permeate was determined by chemical oxygen demand (COD).

2. Experimental

2.1. Membrane preparation

PVDF high viscosity Solef® 1015 supplied by Solvay Belgium, and PMMA purchased from Aldrich (MW = 101 000 g/mol) were used for preparing asymmetric membranes. All the membranes have a total solid concentration of 17 and 5% PVP K30 additive supplied by Fluka. In Table 1, the different synthesized membranes with different PVDF/PMMA ratio are shown.

Casting solutions were cast on a Viledon 2431 (Carl Freudenberg, Germany) non woven support and

Table 1
Casting solution composition and viscosity

Membrane	PVDF (conc. wt.%)	PMMA (conc. wt.%)	Viscosity (Pa. s)
PVDF	17.0	0	7.72
10PMMA	15.3	1.7	7.09
20PMMA	13.6	3.4	3.52
30PMMA	11.9	5.1	2.46
40PMMA	10.2	6.8	1.43
50PMMA	8.5	8.5	1.04

immersed in bidistilled water at 25 °C. Then membranes were stored in a water bath until being used.

2.2. Contact angle measurements

Contact angle θ, between water and the membrane surface was measured in a 1501 Micromeritics contact anglometer. Each value was obtained 3 min after dropping water on the membrane surface.

2.3. Viscosity measurements

The viscosity measurements of the cast solutions were conducted using a DVIII-Brookfield viscometer at 25 °C.

2.4. Microscopy

The morphology of the membranes was investigated using a JMS-35 JEOL scanning electron microscope. In order to observe the membrane cross section, samples were fractured in liquid nitrogen and coated with gold.

2.5. Filtration experiments

All filtration experiments were carried out in a Minitan-S cell from Millipore. The retentate was circulated on the membrane by a peristaltic pump. The detailed experimental device is similar to report in elsewhere. The experimental protocol is as follows:

For the first 30 min, the membrane was compacted at 100 KPa pressure of transmembrane. Then different pressures from 100 to 20 KPa were applied measuring the corresponding pure water fluxes. Once the hydraulic permeabilities were determined, measurements with dextrans were carried out using a MW ranging from 70 to 4900 KD according to a method reported

in elsewhere [13]. Dextran concentrations were determined using a HPLC from Gilson coupled to a refraction index. The distribution of pore radius can be summarized as follows:

$$f_d = \frac{d(J_{w,t}/J_w)}{d(r_p)} \tag{1}$$

where f_d is the differential flux fraction, $J_{w,t} = J_v (1 - R)$, J_v is permeate flux, R the dextrans retention coefficient, and $J_w = J_v - J_s$ with $J_s = J_v C_p$. C_p is dextran concentration in permeate side. r_p can be related to the molecular size of dextran molecule by

$$r_p = 0.4253 \, (MW)^{0.45} \tag{2}$$

Once measurements were carried out, the membrane was mechanical cleaned with pure water for 1 h, then the fouling test experiments with oil emulsion were performed. The emulsion from an engine factory with 5% oil/water concentration was diluted up to 0.1% oil/water concentration. The emulsion had $2.0 \pm 0.5 \, \mu m$ diameter of average oil droplet size measured by a Carl Zeiss Pol II microscope.

2.6. Chemical oxygen demand (COD)

A sample was refluxed in strongly acid solution with a predetermined excess of potassium dichromate. Consumed oxygen was measured against standards at 600 nm by U-2001 UV-Vis Hitachi spectrophotometer. (5220D Standard Method for the Examination of Water and Wastewater).

3. Results and discussion

3.1. Membrane hydrophilicity

The contact angle is an important parameter in surface sciences. It is a regular measure of the surface hydrophobicity [14–16]. Table 2 shows values of contact angle and hydraulic permeabilities of the obtained membranes. The values of contact angle for pure polymers coincide relatively well with those reported by other authors [17] and denote both the hydrophilic character of PMMA related to the contributions dipole–dipole and induced dipole–dipole, and the hydrophobic character of PVDF related to the interaction of Van der Waals.

Table 2
Values of contact angle, hydraulic permeability and mean pore radii

Membrane	Contact angle θ	Lhi $\times 10^9$ (m^3/m^2 Pa s)	r_{pm} (nm)
PVDF	84	1.44	31.90
10PMMA	70	2.56	28.70
20PMMA	68	1.73	25.80
30PMMA	66	2.55	27.20
40PMMA	66	1.70	22.60
50PMMA	64	1.21	24.60
PMMA	58.00	–	–

3.2. Membrane mean pore sizes

Dynamic mean pore radii (r_{pm}) were obtained from pore size distributions by permeation of polydispersed solutes (Fig. 1). This figure shows that the obtained membranes have pore size distributions between 10 and 60 nm and there is a considerable population of pores with radii larger than r_{pm}.

3.3. Membrane hydraulic permeabilities

From the gathered data, a net effect of the PMMA increase on the structure characteristics of prepared membranes cannot be elucidated. Nunes and Peinemann [1] reported an increase of hydraulic permeability values with a PMMA increase ranging from 0.5 to 5% when using a 19% PVDF membrane. However, for the membrane obtained with 19% of PVDF and 10% of PMMA, values of Lhi and retention decrease considerably. The SEM images indicated that as the amount of PMMA increased the membrane thickness and the number and size of macrovoids increased as well. It is worth noting that precursor solutions prepared by these authors have an increasing amount of solids (PVDF/PMMA) in the casting solution. Thus, this behavior was related to the increase of polymeric mass in the casting solution. In the system studied in this work instead, the polymeric mass remains constant. From the SEM photographs given in Figs. 2 and 3, the structure change of membranes can be observed. Only the PVDF and 50PMMA micrographs representing the most extreme structures are shown. It can be seen how the membrane structure varies increasing the presence of macrovoids when PMMA content is 50% of the total polymeric mass. Values of permeability and pore radius do not vary greatly and this stable trend is showing that pore generation on the surface can be attributed to 17% total polymeric
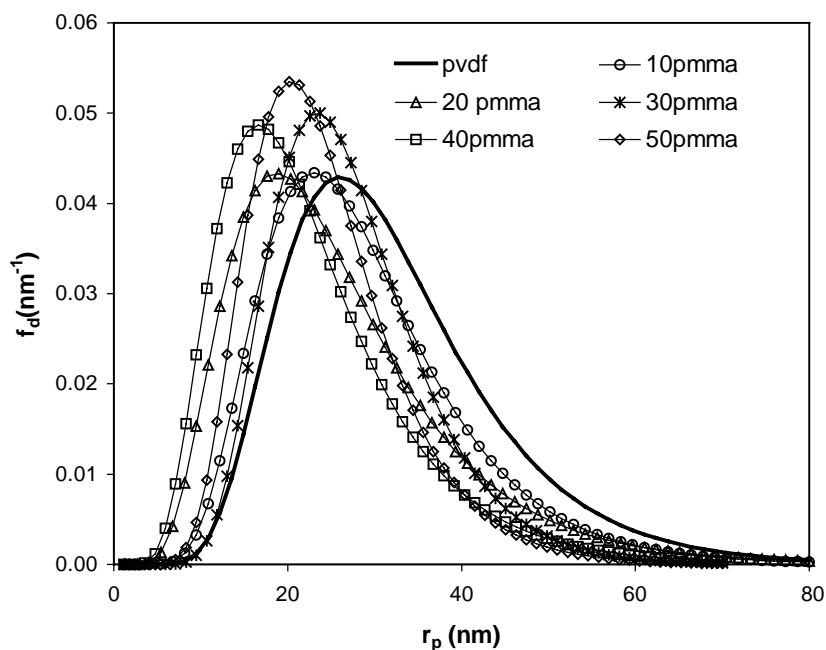

Fig. 1. Normalised differential pore size distribution for the membranes studied, attending to flow, obtained by retention experiments.
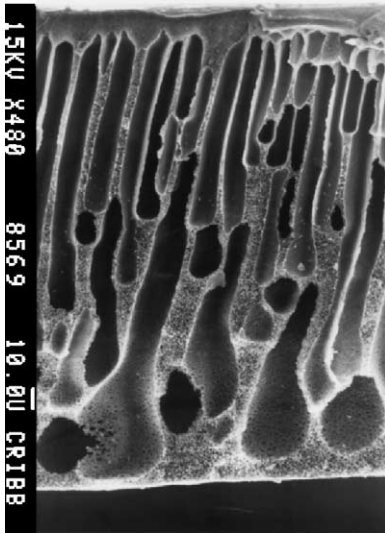
Fig. 2. Cross section structure of PVDF membrane.

Fig. 4. Water flux at 50 KPa transmembrane pressure.

mass and to the presence of 5% additive for all synthesized membranes. However, there is a decrease of the permeability value for 50PMMA membrane. This effect can be attributed to the compaction of prepared membranes. Compaction is an effect also observed by other authors in a wide variety of membrane materials [18–20]. It appears when a polymeric m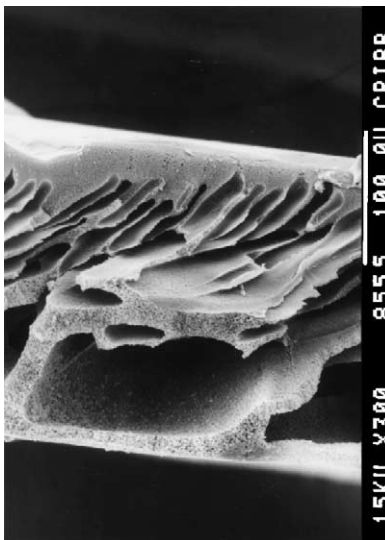embrane undergoes pressure, the polymers are slightly reorganized and the structure is changed, resulting in lowered volume porosity, increased membrane resistance and eventually lowered flux.

Fig. 4 shows the effect of compaction on PVDF-PMMA synthesized membranes measured at a transmembrane pressure of 50 000 Pa. The permeation studies do not show a methodical change with PMMA content. This behavior can be accounted for by analyzing the influence of the increase amount of PMMA upon the compaction, hydrophilicity and surface porosity of the synthesized membranes. Here, the compaction, hydrophilicity and surface porosity will increase. An increase in hydrophilicity and surface porosity leads to an increase of water permeability, while an increase in compaction conveys to a decrease on water flux. These opposing effects result in a non-systematic change of hydraulic permeability (or membrane resistance) with the amount of PMMA.

The membrane compaction effect can be modeled by expressing the membrane resistance term two-fold: Rmc as unaffected constant term and Rmv as pressure dependent, hence it can be written:

$$\frac{\Delta P}{\mu J_i} = \text{Rmc} + \text{Rmv} = \text{Rm} \tag{3}$$

where ΔP is the transmembrane pressure, μ is the viscosity of pure water and J_i is the flux of pure water. Rmv defines the additional resistance caused by an increased pressure due to the hydrodynamic compaction. It is a phenomenological relationship, not based on any special theory [20].

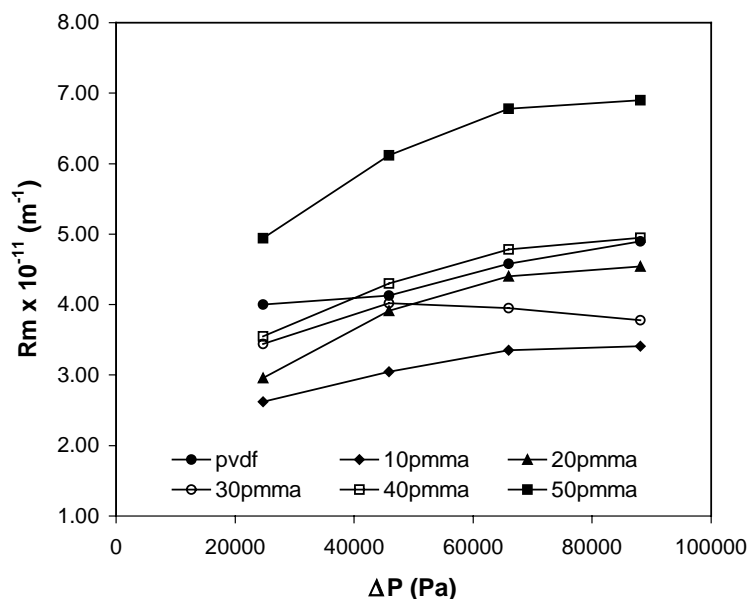Fig. 3. Cross section structure of 50PMMA membrane.

Fig. 5. Changes in membrane resistances as a function of applied pressure.

The membrane deformation can be either reversible or irreversible, depending on the level of molecular rearrangement. The study of total resistance enhances the variation of R_{mv} at transmembrane pressure corresponding to the reversible compaction effect since membranes have been previously compacted (100 KPa). A membrane not affected by compaction should result in a pressure independent resistance. The obtained data are shown in Fig. 5.

The results clearly indicate the effect of reversible compaction undergone by all the prepared membranes. This leads to an increase of the membrane resistance by the effect of pressure. This effect can be observed in 50PMMA membrane where a considerable increase in the resistance value is found. With respect to this membrane, a higher resistance is generated and a higher variation of R_m values by pressure is found. In 40PMMA membrane, a similar effect can be observed. In PVDF membrane and those with low content of PMMA, it is worth noting that pressure does not have a great influence on the resistance. Considering that pore values of these membranes and hydraulic permeability values found in the membranes after compaction are similar, the results would indicate a decrease of water flux due to the effect of transmembrane pressure that compacts the mem-

branes. As PMMA presence grows in the membrane, the effect of this compaction is due to the presence of macrovoids in the membrane porous substructure as mentioned by Nunes and Peinemann [1]. The presence of the second more hydrophilic polymer in the solution may also contribute to an increase in fluctuations, promoting areas of weaker interfacial tension for the entrance of water and consequently formation of cavities. The effects of macrovoids can also be expected considering the decrease in viscosity values of casting solutions shown in Table 1. A similar effect of macrovoid generation due to the decrease of viscosity of polymer solutions can be obtained when solutions with different polymer concentrations are cast [21].

3.4. Fouling measurements

Membrane fouling is a complex phenomenon where permeate flux declines drastically due to phenomena involving chemical and physical factors [22,23].

The flux drop can be summarized as follow [24]:

$$J_v = \frac{1}{A}\frac{\mathrm{d}V}{\mathrm{d}t} = J_{v,0}(1 + Kt)^n \tag{4}$$

where J_v is the permeate flux, A the effective area of membrane, V the permeate total volume, t time, $J_{v,0}$

initial flux of the resulting dynamic membrane after the blocking of initial pores [25].

For the cake model, $n = 2$ and

$$K \equiv 2K_{CF}J_{v,0}^2 \tag{5}$$

with

$$K_{CF} = C_{CF}\frac{\rho_c\eta}{\Delta P} \tag{6}$$

where ρ_c is the cake mass per unit of permeate volume, η is the feed solution viscosity ($\eta = 1.58 \times 10^{-3}$ Pa. s) and C_{CF} is the apparent specific resistance of the cake. To calculate C_{CF}, it has been assumed that the deposited mass per unit of filtered volume, ρ_c, is equal to the feed oil/water concentration. In fact it is strictly true only for dilute concentrations [13,18]. An integration of Eq. (4) leads to:

$$\frac{t}{V} = K_{CF}V + \frac{1}{J_{v,0}} \tag{7}$$

where t is the time (s), and V is the permeate volume until time t per surface unit of membrane (m).

The measurements of flux decline with the oil–water emulsions are shown in Fig. 6. This figure indicate a sharp decrease of permeate flux as a function of time. Considering the mean pore size of these membranes
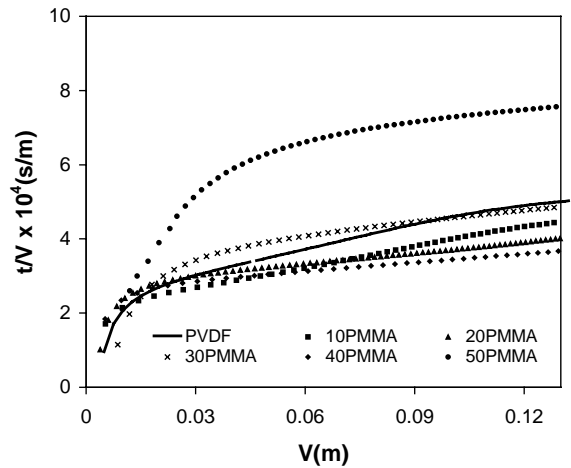

Fig. 7. t/V as a function of V fitted to the cake filtration model.

and the $2\,\mu m$ average drop size of the emulsion, it can be assumed that the high rejection of particles generates a cake layer in a few minutes.

Fig. 7 show the representation of experimental data according with the filtration cake model (Eq. (7)). The K_{CF} and $J_{v,0}$ parameters obtained by linear least square regression analysis of the t/V data are shown
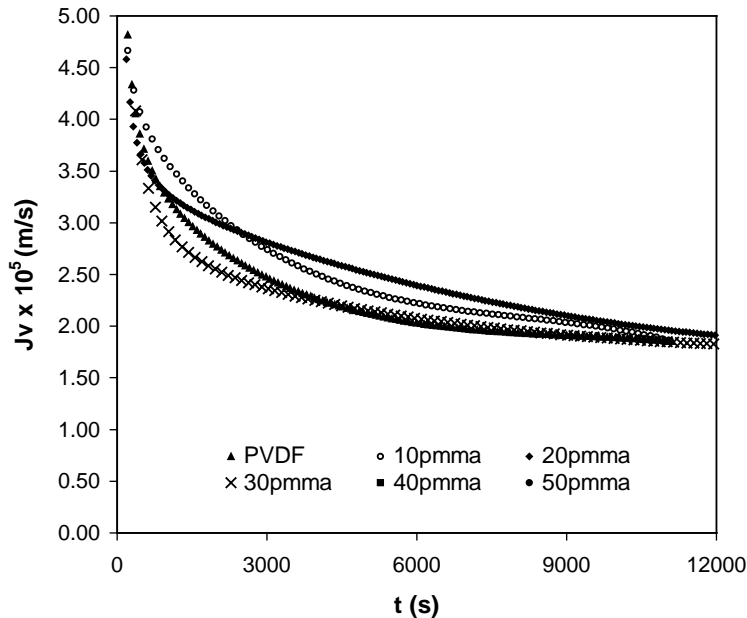

Fig. 6. Permeate flux decline for the different membranes studied measured at 50 KPa transmembrane pressure.

Table 3
Cake model parameters

Membrane	$K_{CF} \times 10^5$ (s/m^2)	$J_{v,0} \times 10^5$ (m/s)	$C_{CF} \times$ 10^{-15} (m/g)
PVDF	4.47	4.20	14.14
10PMMA	3.74	4.74	11.83
20PMMA	2.22	3.83	7.02
30PMMA	2.05	2.83	6.48
40PMMA	1.55	3.76	4.90
50PMMA	1.24	1.47	3.92

Table 4
COD measurements

Membrane	COD of permeate (ppm)
PVDF	272
10PMMA	172
20PMMA	132
30PMMA	146
40PMMA	107
50PMMA	89

COD feed emulsion: 935 ppm.

in Table 3. The range of straight-line portion of the curves selected in the linear regression covers the t/V values with a standard deviation no more than 0.995.

Values of $J_{v,0}$ are also very similar for all membranes. It is evidently lower than water permeate flux, as far as it corresponds to the resulting dynamic membrane after initial blocking process of pores. Similar results were found by other authors [25]. The effect on 50PMMA membrane due to compaction is clearly observed. In it, a lower permeate flux compared to the other prepared membranes can be observed.

However, with respect to K_{CF} values, it can be observed that the time constant of cake model decreases as PMMA increases in the casting solution. This phenomenon is closely related to the growing hydrophilicity of membranes, taking into account both pore radius distribution and Lhi values of the obtained membranes. Marchese et al. [13] analyzed the effect of PVP additive presence on fouling with BSA in PES membranes. A decrease of K_{CF} values was found in membranes prepared with the additive having all the samples under study similar pore sizes.

In the present work, the effect of hydrophilicity directly related to the presence of PMMA produces a reduction of the fouling rate (K_{CF}). This significant change of flux rate is reflected in the apparent specific cake resistance values determined by Eq. (6). In Table 3, a decrease of C_{CF} as the PMMA content increases is shown. These results indicate that a less compact layer cake is formed due to a lower adsorption of oil molecules on the membrane surface according with the growing hydrophilic character of membranes.

The quality of permeate was determined by COD as shown in Table 4. The COD measurement value for feed emulsion was 935 ppm.

In Table 4, it can be observed that those membranes with a higher hydrophilic character have higher oil rejection. Therefore, the rejection is affected not only by pore radius distribution of membrane but also by the solute-membrane interaction. This effect is observed in the 50PMMA membrane, which has a better permeate quality than that of membranes with similar mean pore sizes. Similar results were found by Castro et al. [26] when a hybrid ceramic-polymeric membrane was developed by the growth of covalently-bonded polyvinylpyrrolidone (PVP) chains from the surface of a porous silica support membrane since this membrane produced a lower permeate concentration at an equivalent permeability. The improved selectivity and reduced fouling tendency was attributed to the increased hydrophilicity of the membrane surface provided by the grafted PVP chains.

4. Conclusions

Membranes with growing hydrophilic character from PVDF/PMMA blends were synthesized by the phase-inversion process. The hydrophilicity was corroborated by contact angle measurements. Increasing the PMMA content in the blends, membranes with similar mean pore radii (22–32 nm) and hydraulic permeabilities were obtained. However, macrovoids of higher size and with higher frequency appeared in the porous substructure below the selective surface, as the PMMA content was increased. These macrovoids produced a collapse of membrane structure due to the compaction that the pressure of this type of process produces. This brings about a 50%-PMMA membrane with a lower value of permeability.

The cake model was used to evaluate the drop of membrane flux. It was found that a higher hydrophilic character produces a lower rate of membrane fouling. This leads to a decrease of the apparent cake

resistance as the content of PMMA in the membrane increases. From the determinations of the permeate quality, it is observed that the sieving effect of a membrane is not only determined by pore size but also by the hydrophilic–hydrophobic property character of a membrane. The COD values of permeate are within the allowed values for its direct unloading to the municipal treatment plants according to San Luis Province legislation [27].

References

[1] S.P. Nunes, K.V. Peinemann, Ultrafiltration membranes from PVDF/PMMA blends, J. Membr. Sci. 73 (1992) 25–35.

[2] T. Uragami, M. Fujimoto, M. Sugihara, Studies on synthesis and permeabilities of special polymer membranes. 28. Permeation characteristics and structure of interpolymer membranes from poly(vinilydene fluoride) and poly(styrene sulfonic acid), Desalination 34 (1980) 311–323.

[3] Z.L. Xu, T.S. Chung, K.C. Loh, B.C. Lim, Polymeric asymmetric membranes made from polyetherimide/polbenzimidazole/poly(ethylene glycol) (PEI/PBI/PEG) for oil-surfactant-water separation, J. Membr. Sci. 158 (1999) 41–53.

[4] J.F. Hester, A.M. Mayes, Design and performance of foul-resistant poly(vinylidene fluoride) membranes prepared in a single-step by surface segregation, J. Membr. Sci. 202 (2002) 119–135.

[5] P. Wang, K.L. Tan, E.T. Kang, K.G. Neoh, Plasma-induced immobilization of poly(ethylene glycol) onto poly(vinylidene fluoride) microporous membrane, J. Membr. Sci. 195 (2002) 103–114.

[6] S.P. Nunes, M.L. Sforça, K.V. Peinemann, Dense hydrophilic composite membranes for ultrafiltration, J. Membr. Sci. 106 (1995) 49–56.

[7] M. Sforça, S.P. Nunes, K.V. Peinemann, Composite nanofiltration membranes prepared by in situ polycondenation of amines in a poly(ethylene oxide-*b*-amide) layer, J. Membr. Sci. 135 (1997) 179–186.

[8] T. Kanamori, K. Sakai, M. Fukuda, Y. Yamashita, Preferable structure of poly(ethylene glycol) for grafting onto a cellulosic membrane to increase hemocompatibility without reduction in solute permeability of the membrane, J. Appl. Polym. Sci. 55 (1995) 1601–1605.

[9] H. Chen, G. Belfort, Surface modification of poly(ether sulfone) ultrafiltration membranes by low-temperature plasma-induced graft polymerization, J. Appl. Polym. Sci. 72 (1999) 1699–1711.

[10] K.J. Kim, A.G. Fane, C.J.D. Fell, The performance of ultrafiltration membranes pretreated by polymers, Desalination 70 (1988) 229–249.

[11] S.T. Kelly, A.L. Zydney, Mechanisms for BSA fouling during microfiltration, J. Membr. Sci. 107 (1995) 115–127.

[12] J. Mueller, R.H. Davis, Protein fouling of surface-modified polymeric microfiltration membranes, J. Membr. Sci. 116 (1996) 47–60.

[13] J. Marchese, P. Pradanos, N.A. Ochoa, M. Ponce, L. Palacio, A. Hernandez, Fouling behaviour of polyethersulfone UF membranes made with different PVP, J. Membr. Sci. 211 (2003) 1–11.

[14] J.T.F. Keurentjes, J.G. Harbrecht, D. Brinkman, J.H. Hanemaajer, M.A. Cohen Stuart, H. van't Riet, Hydrophobicity measurements of MF and UF membranes, J. Membr. Sci. 47 (1989) 333–337.

[15] L. Palacio, J.I. Calvo, P. Pradanos, A. Hernandez, P. Väisänen, M. Nyström, Contact angles and external protein adsorption onto ultrafiltration membranes, J. Membr. Sci. 152 (1999) 189.

[16] W. Zhang, M. Wahlgren, B. Sivik, Membrane Characterization by the contact angle technique. characterization of uf-membranes and comparison between the captive bubble and sessile drop as methods to obtain water contact angles, Desalination 72 (1989) 263–273.

[17] K. Feldman, T. Terwoort, P. Smith, N. Spencer, Toward a force spectroscopy of polymer surfaces, Langmuir 14 (1998) 372–378.

[18] E. Tracey, R. Davis, Protein fouling of track-etched polycarbonate microfiltration membranes, J. Colloid Interface Sci. 167 (1994) 104–116.

[19] J. Mueller, Y. Cen, R.H. Davis, Crossflow microfiltration of oily water, J. Membr. Sci. 129 (1997) 221–235.

[20] K.M. Persson, V. Gekas, G. Trägardh, Study of membrane compaction and its influence on ultrafiltration water permeability, J. Membr. Sci. 100 (1995) 155–162.

[21] R. Kesting, Synthetic Polymeric Membranes, second ed., Wiley, 1985.

[22] G. Belford, R.H. Davis, A.L. Zydney, The behavior of suspensions and macromolecular solutions in crossflow microfiltration, J. Membr. Sci. 96 (1994) 1–58.

[23] A.D. Marshall, P.A. Munro, G. Tragardh, The effect of protein fouling in microfiltration and ultrafiltration on permeate flux, protein retention an selectivity: a review, J. Membr. Sci. 91 (1993) 65–108.

[24] C. Herrero, P. Prádanos, J.I. Calvo, F. Tejerina, A. Hernández, Flux decline in protein microfiltration: influence of operative parameters, J. Colloid Interface Sci. 187 (1997) 344–350.

[25] P. Pradanos, A. Hernandez, J.I. Calvo, F. Tejerina, Mechanisms of protein fouling in cross-flow UF through an asymmetric inorganic membrane, J. Membr. Sci. 114 (1996) 115–126.

[26] R.P. Castro, Y. Cohen, H.G. Monbouquette, Silica-supported polyvinylpyrrolidone filtration membranes, J. Membr. Sci. 115 (1996) 179–190.

[27] Law 5042 "Dangerous Waste Treatment". Government of San Luis Province, 1995.